PARAMETRIC OPTIMIZATION FOR CLOSE-APPROACH TRAJECTORIES

IAF-00-A.4.07

Gislaine de Felipe
Antonio Fernando Bertachini de Almeida Prado
Instituto Nacional de Pesquisas Espaciais
São José dos Campos - SP - 12227-010 - Brazil

ABSTRACT

The swing-by maneuver is a technique used to reduce the fuel consumption of space missions. It uses a close approach with a celestial body to modify the velocity, energy and angular momentum of a spacecraft. The literature has several papers studying this problem, usually using a patched-conic approximation. In the present paper the swing-by maneuvers are studied and classified under the model given by the restricted three-body problem. To show the results, the orbits of the spacecraft are classified in four groups: elliptic direct, elliptic retrograde, hyperbolic direct and hyperbolic retrograde. Then, the modification in the orbit of the spacecraft due to the close approach is shown in plots that specify from which group of orbits the spacecraft is coming and to which group it is going. The results generated here are used to solve optimal problems, such as finding trajectories that satisfy some given constraints (such as achieving an escape or a capture) with some parameters being extremized (position, velocity, etc...).

INTRODUCTION

The literature shows several applications of the swing-by technique. Some of them can be found in Swenson[1], that studied a mission to Neptune using swing-by to gain energy to accomplish the mission; Weinstein[2], that made a similar study for a mission to Pluto; Farquhar and Dunham[3], that formulated a mission to study the Earth's geomagnetic tail; Farquhar, Muhonen and Church[4], Efron, Yeomans, and Schanzle[5] and Muhonen, Davis, and Dunham[6], that planned the mission ISEE-3/ICE; Flandro[7], that made the first studies for the Voyager mission; Byrnes and D'Amario[8], that design a mission to flyby the comet Halley; D'Amario, Byrnes and Stanford[9,10] that studied multiple flyby for interplanetary missions; Marsh and Howell[11] and Dunham and Davis[12] that design missions with multiple lunar swing-bys; Prado and Broucke[13], that studied the effects of the atmosphere in a swing-by trajectory; Striepe, and Braun[14], that used a swing-by in Venus to reach Mars; Felipe and Prado[15], that studied numerically a swing-by in three dimensions, including the effects in the inclination; Prado[16], that considered the possibility of applying an impulse during the passage by the periapsis; Prado and Broucke[17], that classified trajectories making a swing-by with the Moon. The most usual approach to study this problem is to divide the problem in three phases dominated by the "two-body" celestial mechanics. Other models used to study this problem are the circular restricted three-body problem (like in Broucke[18], Broucke and Prado[19], and Prado[20]) and the elliptic restricted three-body problem (Prado[21]).

The objective is to simulate a large variety of initial conditions for swing-by trajectories and classify them according to the effects caused by the close approach in the orbit of the spacecraft. This swing-by is assumed to be performed around the secondary body of the system. The equations of motion are integrated numerically forward and backward in time, until the spacecraft is at a distance that can be considered far enough from M_2. It is necessary to integrate in both directions of time because the set of initial conditions used gives information about the spacecraft exactly at the moment of the closest approach. At these two points, the effect of M_2 can be neglected and the system formed by M_1 and the spacecraft can be considered a two-body system. At these two points, two-body celestial mechanics formulas are valid to compute the energy and the angular momentum before and after the close approach. With those results, the orbits are classified in four categories: elliptic direct (negative energy and positive angular momentum), elliptic retrograde (negative energy and angular momentum), hyperbolic direct (positive energy and angular momentum) and hyperbolic retrograde (positive energy and negative angular momentum). Then, the problem is to identify the category of the orbit of the spacecraft before and after the close encounter with M_2. After that, those results are used to identify up to sixteen classes of transfers, accordingly to the changes in the category of the

orbit caused by the close encounter. They are named with the first sixteen letters of the alphabet. After that, several optimal problems involving this maneuver can be formulated and solved with the help of the plots shown. Some examples include finding specific types of orbits (escape, capture, etc.) that have maximum or minimum velocity at periapsis (or any other parameters, such as the distance of the periapsis or the angle of approach).

THE PATCHED-CONICS APPROACH

This section explains the patched conics approach of the swing-by maneuver. The simple model of two-bodies is used for each part of the mission. This material is largely based on Broucke[18]. It is assumed that the system is formed by three bodies: M_1, a massive body in the center of the Cartesian system; M_2, a planet or satellite of M_1, that is a smaller body in a Keplerian orbit around M_1; M_3, a massless spacecraft or particle orbiting M_1, when it makes a close approach with M_2. This close approach changes the orbit of M_1, and this is what is called a "swing-by" maneuver. Under those hypotheses, the orbit of M_1 and M_2 are not changed by this close approach. Fig. 1 describes this event and shows some of the variables involved.

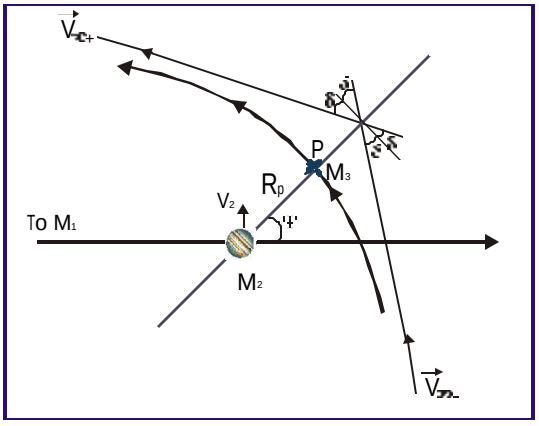

Fig.1 - The swing-by Maneuver and its variables.

The variables are: $\vec{V}_2$ = the velocity of M_2 relative to M_1; $\vec{V}_\infty^-, \vec{V}_\infty^+$ = vector velocities of the spacecraft relative to M_2 before and after the close encounter; $\vec{V}_i, \vec{V}_o$ (see Fig.2) = vector velocities of the spacecraft relative to M_1 before and after the close encounter, in the inertial frame; δ = half of the bending angle (the angle between $\vec{V}_\infty^-$ and $\vec{V}_\infty^+$); R_p = the distance of the closest approach (point P) between M_2 and M_3; ψ = the angle between the periapsis line (the line connecting M_2 to P) and the M_1-M_2 line. To find the equations needed, it is necessary first to go to the theory of hyperbolic orbits to get an expression for δ. This expression is:

$$\sin(\delta) = \frac{1}{1+\frac{R_p V_\infty^2}{\mu_2}} \qquad (1)$$

where $\mu_2 = Gm_2$, with G the gravitational constant.

From this equation and the last figure, it is possible to identify that the independent variables that describe completely the swing-by maneuver are the following:

i) $\left|\vec{V}_\infty\right|$, the magnitude of the velocity of the spacecraft at infinity. The variable V_p is equivalent in the approach used to derive those equations (patched conics), because the orbit around of M_2 is considered Keplerian (Hyperbolic). The parameters are related by the expression: $V_\infty^2 = V_p^2 - \frac{2\mu}{R_p}$;

ii) R_p, the periapsis distance;

iii) ψ, the angle of approach.

The "patched conics" approximation has three phases:

i) In the first one M_2 is neglected and the motion of M_3 around M_1 is considered a Keplerian orbit;

ii) In the second phase, it is assumed that M_3 is entering the sphere of influence of M_2. Then, the velocity $\vec{V}_\infty^-$ is calculated, from the equation $\vec{V}_\infty^- = \vec{V}_i - \vec{V}_2$ and the effect of M_1 is neglected. The motion of M_3 around M_2 is hyperbolic in the case of interest for the present research. In this hyperbolic orbit the spacecraft M_3 is scattered by M_2 and its velocity vector (with respect to M_2) rotates by an angle 2δ, but it keeps its magnitude constant. Then the spacecraft crosses again the sphere of influence of M_2 and leaves it, to return to a Keplerian orbit around M_1. At this point, the velocity $\vec{V}_\infty^+$ is given by $\vec{V}_\infty^+ = \vec{V}_o - \vec{V}_2$;

iii) After that the spacecraft is in a new Keplerian orbit around M_3 and the swing-by is complete.

The study of the differences between the orbits before and after this close encounter (steps i and iii) and some of its applications are studied here.

The first important quantity calculated is the $\Delta\vec{V} = \vec{V}_o - \vec{V}_i$, the difference between the inertial velocities before and after the swing-by. From a

diagram of vector addition, it is possible to know that (see Fig. 2):

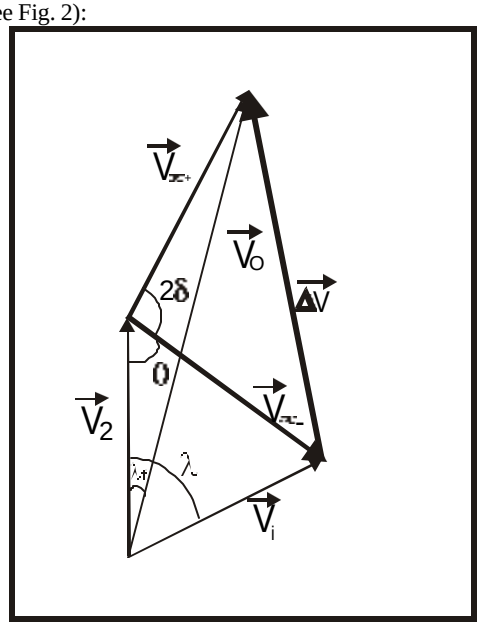

Fig. 2 - Additions of the velocity vectors

$$\Delta V = \left|\Delta\vec{V}\right| = 2\left|\vec{V}_\infty\right|\sin(\delta) = 2V_\infty\sin(\delta) \qquad (2)$$

and that $\Delta\vec{V}$ makes an angle ψ+180° with the M_1-M_2 line. This fact gives the following components for the increment in velocity (see Fig. 3).

$$\Delta\dot{X} = -2V_\infty\sin(\delta)\cos(\psi) \qquad (3a)$$

$$\Delta\dot{Y} = -2V_\infty\sin(\delta)\sin(\psi) \qquad (3b)$$

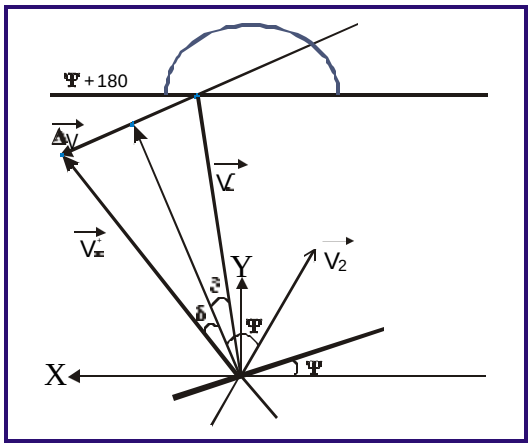

Fig. 3 - Velocity vectors.

The second important quantity is the angular momentum C. From its definition it is possible to get the expression $C = X\dot{Y} - Y\dot{X}$, what gives the equation $\Delta C = X\Delta\dot{Y} + \Delta X\dot{Y} - Y\Delta\dot{X} - \Delta Y\dot{X}$ for its first variation. This equation becomes $\Delta C = d\Delta\dot{Y}$, under the assumptions that the close approach is instantaneous ($\Delta X = \Delta Y = 0$) and that at t = 0, X = d and Y = 0. Then, combining this result with the expression for $\Delta\dot{Y}$ (equation 3b) the result is:

$$\omega\Delta C = -2V_2V_\infty\sin(\delta)\sin(\psi) \qquad (4)$$

The third and last quantity derived here is the change in energy. This is done by directly subtracting the energy after the close approach E_+ $\left(=\frac{1}{2}\left[\left(\dot{X}+\Delta\dot{X}\right)^2+\left(\dot{Y}+\Delta\dot{Y}\right)^2\right]\right)$ from the energy before $E_-\left(=\frac{1}{2}\left(\dot{X}^2+\dot{Y}^2\right)\right)$. The result is:

$$\Delta E = E_+ - E_- = 2V_\infty\sin(\delta)\left[V_\infty\sin(\delta) - \left(\dot{X}\cos(\psi) + \dot{Y}\sin(\psi)\right)\right] \qquad (5)$$

This equation can be simplified (Broucke[18]) to:

$$\Delta E = -2V_2V_\infty\sin(\delta)\sin(\psi) \qquad (6)$$

Looking at equations (4) and (6), a fundamental result can be found. It is:

$$\Delta E = \omega\Delta C \qquad (7)$$

Some important consequences of these equations can be derived by studying equation (6) in more details. The parameters V_2 and V_∞ are positive quantities (they are the magnitude of two vectors), as well as sin(δ) (because 0° < δ < 90°). Then, the only parameter that affects the sign of ΔE is sin(ψ). The conclusion is that for values of ψ in the range 0° < ψ < 180°, ΔE is negative (decrease in energy) and for ψ in the range 180° < ψ < 360°, ΔE is positive (increase in energy).

Then, the final conclusions are: if the swing-by is in front of M_2 there is a decrease in the energy of M_3, with a maximum loss at ψ = 90° ($\Delta\vec{V}$ opposite to $\vec{V}_2$); if the swing-by is behind M_2 there is an increase in the energy of M_3, with a maximum gain at ψ = 270° ($\Delta\vec{V}$ aligned with $\vec{V}_2$).

THE RESTRICTED PROBLEM OF THREE BODIES

For the research performed in this paper, the equations of motion for the spacecraft are assumed to be the ones valid for the well-known restricted circular three-body problem. The standard dimensionless canonical system of units is used, which implies that: the unit of distance is the distance between M_1 and M_2; the mean angular velocity (ω) of the motion of M_1 and M_2 is assumed to be one; the mass of the smaller primary (M_2) is given by $\mu = m_2/(m_1 + m_2)$ (where m_1 and m_2 are the real masses of M_1 and M_2, respectively) and the mass of M_2 is (1-μ); the unit of time is defined such that the period of the motion of the two primaries is 2π and the gravitational constant is one. There are several systems of reference that can be used to describe the restricted three-body problem[22]. In this paper the rotating system is used. In this system of reference, the origin is the center of mass of the two massive primaries. The horizontal axis (x) is the line that connects the two primaries at any time. It rotates with a variable angular velocity in a such way that the two massive primaries are always on this axis. The vertical axis (y) is perpendicular to the (x) axis. In this system, the positions of the primaries are: $x_1 = -\mu$, $x_2 = 1-\mu$, $y_1 = y_2 = 0$. In this system, the equations of motion for the massless particle are[22]:

$$\ddot{x} - 2\dot{y} = x - (1-\mu)\frac{x+\mu}{r_1^3} - \mu\frac{x-1+\mu}{r_2^3} \quad (8a)$$

$$\ddot{y} + 2\dot{x} = y - (1-\mu)\frac{y}{r_1^3} - \mu\frac{y}{r_2^3} \quad (8b)$$

where r_1 and r_2 are the distances of M_1 and M_2, given by:

$$r_1 = ((x+\mu)^2 + y^2)^{1/2} \quad (9)$$

$$r_2 = ((x-1+\mu)^2 + y^2)^{1/2} \quad (10)$$

ALGORITHM

With those equations, it is possible build a numerical algorithm to solve the problem. It has the following steps:

i) Arbitrary values for the three parameters: R_p, V_p, ψ are given;

ii) With these values it is computed the initial conditions in the rotating system. The initial position is the point (X_i, Y_i) and the initial velocity is (V_{Xi}, V_{Yi}), where:

$$X_i = R_p\cos(\psi) + (1-\mu) \quad (11)$$

$$Y_i = R_p\sin(\psi) \quad (12)$$

$$V_{xi} = -V\sin(\psi) \quad (13)$$

$$V_{yi} = +V\cos(\psi) \quad (14)$$

and $V = \sqrt{\dot{x}^2 + \dot{y}^2}$ is calculated from equation that represents the Jacobean constant, given by $J = \frac{1}{2}(\dot{x}^2 + \dot{y}^2) - \frac{1}{2}(x^2 + y^2) - \frac{(1-\mu)}{r_1} - \frac{\mu}{r_2} = \text{Const}$;

iii) With these initial conditions, the equations of motion are integrated forward in time until the distance between M_2 and M_3 is bigger than a specified distance limit d_{lS} (= 0.50). At this point the numerical integration is stopped and the energy (E_+) and the angular momentum (C_+) after the encounter with M_2 are calculated, from the equations:

$$E = \frac{(x+\dot{y})^2 + (\dot{x}-y)^2}{2} - \frac{1-\mu}{r_1} + \frac{\mu}{r_2} \quad (15)$$

$$C = x^2 + y^2 + x\dot{y} - y\dot{x} \quad (16)$$

Remember that it is assumed that the energy and the angular momentum is constant after this point, due to the fact that the perturbation from M_2 is too small to disturb significantly the two-body character of the dynamics. A limit of 10 canonical units of time is also used to stop the integration, if the spacecraft does not reach points A and B;

iv) Then the initial conditions are returned to the point P, and the equations of motion are integrated backward in time, until the distance d_{lS} is reached again. Then the equations (15) and (16) are used to calculate the energy (E_-) and the angular momentum (C_-) before the encounter with M_2;

v) With those results, all the information required to calculate the change in energy ($E_+ - E_-$) and angular momentum ($C_+ - C_-$) due to the close approach are available;

It is necessary to integrate in both directions of time because the set of initial conditions used gives information about the spacecraft exactly at the moment of the closest approach. With those results, the orbits are classified in four categories: elliptic direct, elliptic retrograde hyperbolic direct and hyperbolic retrograde. Then, the problem is to identify the category of the orbit of the spacecraft before and after the close encounter with M_2.

RESULTS

In that way, the results consist of graphs that show the change of the orbit of the space vehicle due to the encounter with M_2 for a large variety of initial conditions. Firstly, it is made the classification of all of the encounters between M_2 and M_3, according to the change obtained in the orbit of the space vehicle.

The letters used are A, B, C, D, E, F, G, H, I, J, K, L, M, N, O and P for this classification. They are related with the orbits according to the rules shown in the table below. The letter Z is used for an orbit that stays captured around M_2 during the whole time of integration.

Table 1: Rules to Assign Letters to Orbits

After: / Before:	Direct Ellipse	Retrograde Ellipse	Direct Hyperbola	Retrograde Hyperbola
Direct Ellipse	A	E	I	M
Retrograde Ellipse	B	F	J	N
Direct Hyperbola	C	G	K	O
Retrograde Hyperbola	D	H	L	P

This diagram type is called letter plot here and it was used previously in Broucke[18] and Prado[20]. In this paper some combinations of R_p and V_p are simulated and shown in Figures 4 and 5. For all the graphs the parameters used are $\mu = 0.00121$ and $d = 0.5$ in canonical units. The interval plotted for Ψ is $180^o < \Psi < 360^o$ because there is a symmetry with respect to the horizontal axis $\Psi = 180^o$. This symmetry comes from the fact that an orbit with an angle $\psi = \theta$ is different from an orbit with an angle $\psi = \theta + 180°$ only by a time reversal. It means that there is a correspondence between these two intervals. This correspondence is: I⇔C, J⇔G, L⇔O, B⇔E, N⇔H, M⇔D. The orbits A, F, K and P are unchanged. With respect to the horizontal axis, the graphs are built with values for R_p fixed and V_p being varied or with fixed values for V_p and R_p being varied.

Results for R_p fixed

In this section graphs are presented where the values of R_p are fixed in 0.00476; 0.00675; 0.009; 0.0225 and 0.045 and the values of V_p are varied inside of the interval $2.0 < V_p < 4.0$, as seen in Fig. 4.

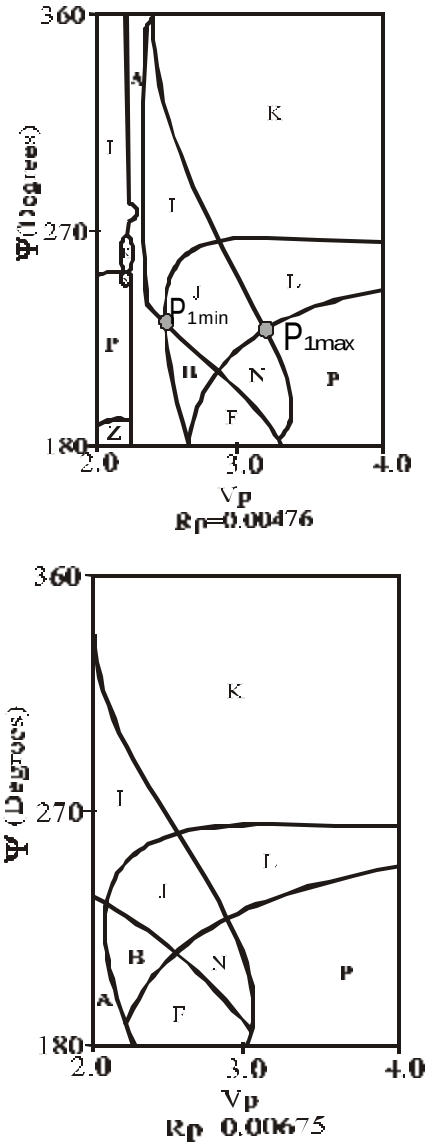

Fig. 4 – Results for R_p fixed

(continue)

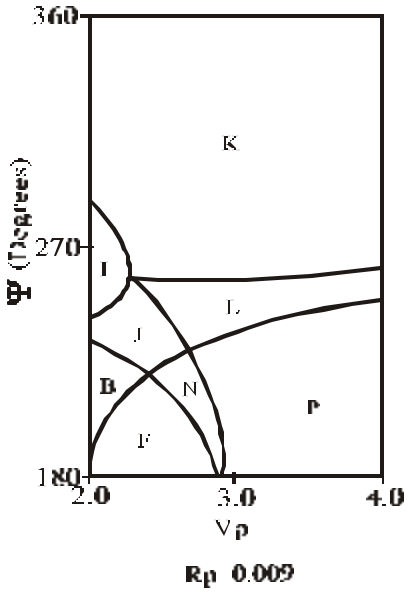

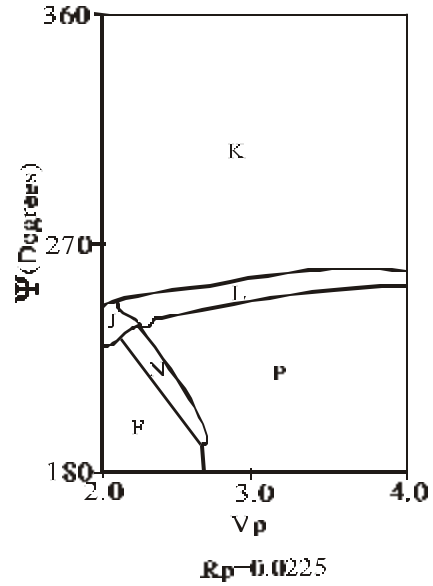

Fig. 4 – Results for R_p fixed

(continue)

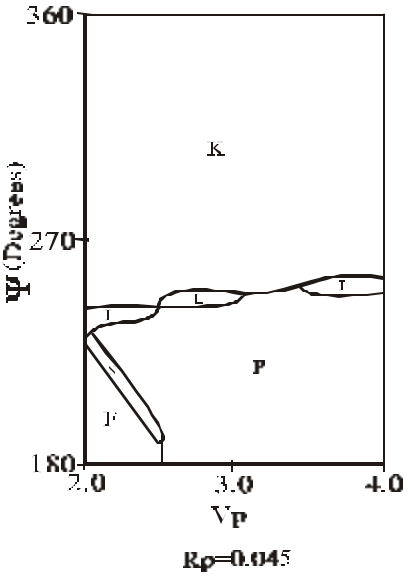

Fig.4 (Conclusion)– Results for R_p fixed

Results for V_p fixed

In this section some graphs are presented where the values of V_p are 2.2; 2.6; 3.0 and 3.4 and the values of R_p are varied in the interval $0.00476 < R_p < 0.045$ (see Fig. 5).

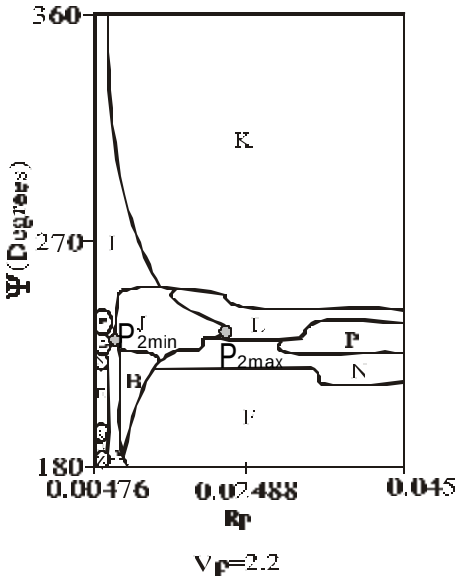

Fig. 5 Results for V_p fixed

(Continue)

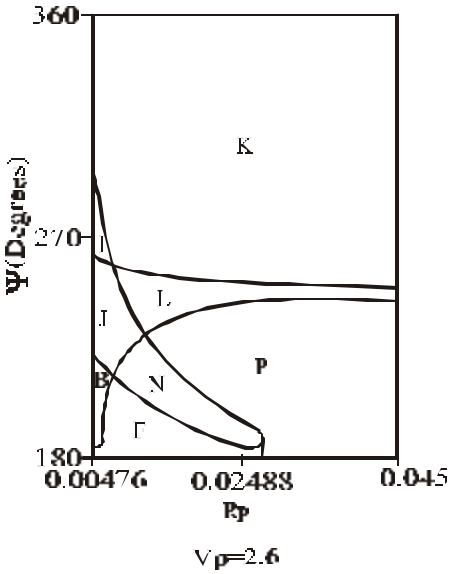

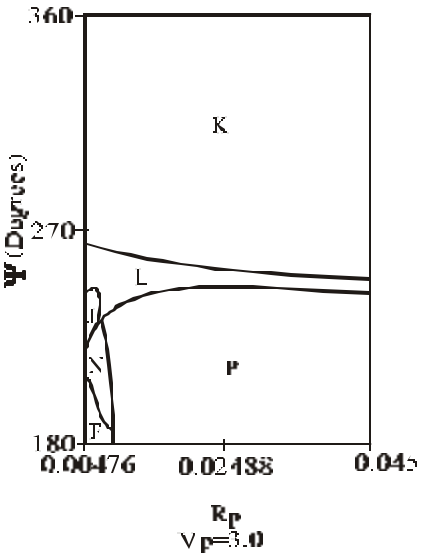

Fig. 5 Results for V_p fixed

(Continue)

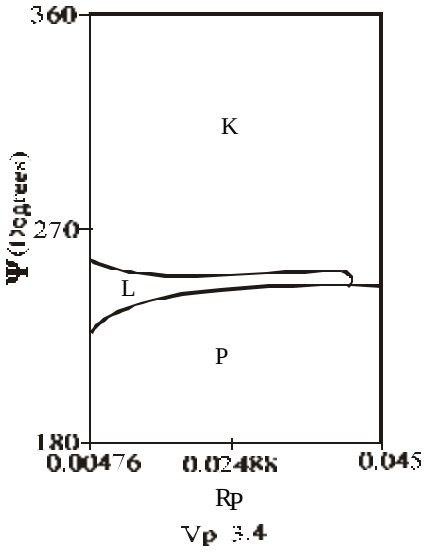

Fig. 5 (Conclusions) - Results for V_p fixed

By examining Figs. 45 it is possible to identify the following families of orbits: a) Orbits that result in an escape (transfer from elliptic to hyperbolic), that are represented by the letters I, J, M, N and that appear between the center ($\psi = 270°$) and the bottom part of some of the plots; b) Orbits that result in a capture (transfer from hyperbolic to elliptic), that are represented by the letters C, D, G, H that do not appear in the plots shown in this paper, except for a single point (but exist in large quantities in the symmetric parts not shown here); c) Elliptic orbits (transfer from elliptic to elliptic), that are represented by the letters A, B, E, F and that appear at the bottom of some of the plots; d) Hyperbolic orbits (transfer from hyperbolic to hyperbolic), that are represented by the letters K, L, O, P and that appears at the upper part of the plots and that are the only families available for higher velocities in the case of R_p fixed; e) Orbits that change the direction of motion from direct to retrograde that are represented by the letters E, M, G, O and that do not appear in the plots shown in this paper except for some scattered points (but exist in large quantities in the symmetric part not shown here; f) Orbits that change the direction of motion from retrograde to direct, that are represented by the letters B, D, J, L, that appear in the lower-center of the plot; g) Retrograde orbits that are represented by the letters F, H, N, P that appear in the majority of the bottom part of the plots; h) Direct orbits that are represented by the letters A, C, I, K that appear in the top of the plots; i).Orbits that stay around M_2 during the time of integration, that are represented by the letter Z that appear at left-bottom of some plots.

The borderlines between those families are also interesting families of orbits. The borders that separate elliptic from hyperbolic orbits are made by parabolic orbits. Examples of borders that have parabolic orbits after the close approach are: A-I, B-J, F-N, F-J, F-P. Examples of borders that have parabolic orbits before the close approach are: I-K, J-L, N-P, K-A, K-J, F-P. It is interesting to see that there is a border that is made by parabolic orbits before and after the close approach. It is the border P-F, that appears, for example, in the case R_p = 0.0225. The borders that separate direct from retrograde orbits are made of orbits with zero angular momentum. It means that the vectors position and velocity are parallel (rectilinear orbits). Examples of borders that have zero angular momentum after the close approach are: F-B, N-J, L-P, P-K, N-L, F-A. Examples of borders that have zero angular momentum before the close approach are: K-L, I-J, A-B, K-P, K-J. Following those examples it is easy to see those families looking at the figures.

Optimal problems

The results generated in this research can be used to help to analyze missions that involve optimization of parameters in a swing-by maneuver. It is possible to use the graphs developed to find situations where a specific case (represented by the letters A-P) can be obtained with one or more variables (like V_p or R_p) extremized. Examples of situations like that are:

1) To collect data from M_2 in the case where there are no threats to the mission. In that case it is desired to minimize R_p (to pass closer of M_2) and/or V_p (to stay more time close to M_2).

2) To execute an orbital change in a planet that represents a risk for the vehicle due to the presence of radiation and/or atmosphere, etc. In that case, it is necessary to maximize V_p and/or R_p, subject to the restriction of obtaining the change desired in the trajectory.

Problem 1

It is desired to obtain a trajectory of Type J (Retrograde Elliptic before and Direct Hyperbolic after) in the Earth-moon system, with R_p = 0.00476 (100 km from the surface) and with maximum or minimum velocity at the perigee. The solutions are in the points P_{1max} and P_{1min} of the Figure 4.

Problem 2

It is desired to obtain a trajectory of Type J (Retrograde Elliptic before and Direct Hyperbolic after) in the Earth-moon system, with free R_p and with minimum velocity at the perigee. It is seen that the optimization happens in the interval $0.0225 < R_p < 0.045$, because the family J exists in R_p = 0.0225 and doesn't exist anymore for R_p = 0.045. Then, Figure 6 is built to solve the problem. It is seen that the solution happens for $0.040 \leq R_p \leq 0.044$, with Ψ = 234° e V_p = 2.0 because this was the established limit in the problem. It is observed that a region solutions exists for R_p and not a single point.

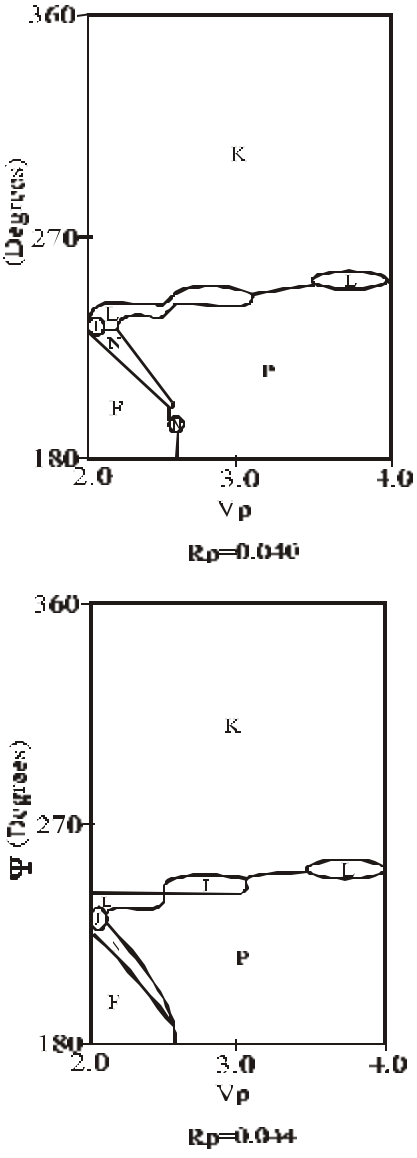

Fig. 6 - Solution of Problem 2

Problem 3

It is desired to obtain a trajectory of Type J (Retrograde Elliptic before and Direct Hyperbolic after) in the Earth-moon system, with V_p = 2.2 and maximum or minimum distance of the perigee. The solutions are in the points P_{2max} and P_{2min} (Figure 5).

Problem 4

It is desired to obtain a trajectory of Type N (Retrograde Elliptic before and Retrograde Hyperbolic after) in the Earth-moon system, with free V_p and to request a minimum perigee distance. It is seen that the optimization happens in the interval $3.0 < R_p < 3.4$, because the family J exists in the case $R_p = 3.0$ and it doesn't exist in the case $R_p = 3.4$. Figure 7 is built to solve the problem. It is seen that the solution happens for $V_p = 3.29$ with $192^o \leq \Psi \leq 204^o$ and $R_p = 0.00476$, because this was the established limit in the problem. It is observed that the solution is not unique in Ψ.

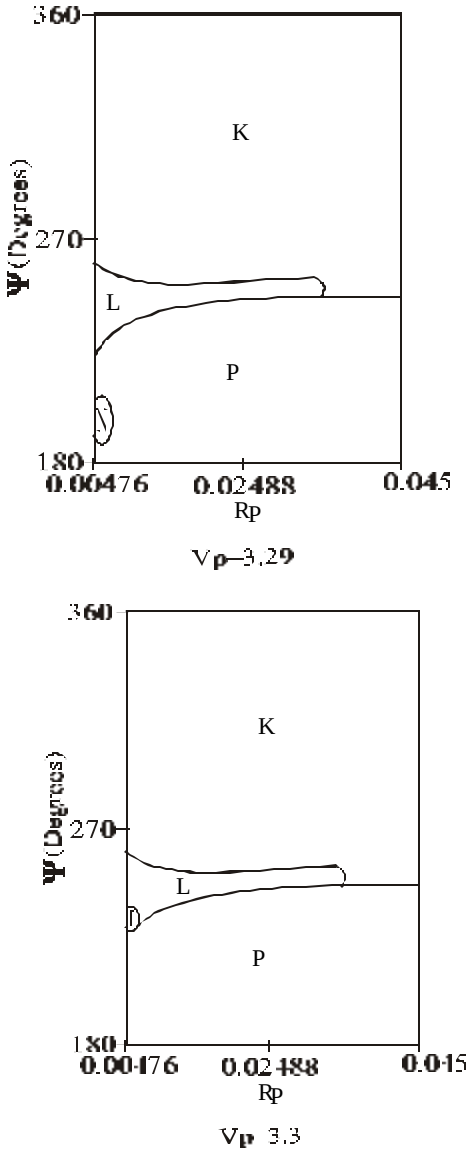

Fig. 7 – Solutions of the Problem 4

CONCLUSIONS

The letter plots represent the effects of the encounter in the orbit of the space vehicle in two dimensions. It is noticed that the hyperbolic orbits (family K) dominate the area $\Psi > 270^o$ and when the velocity increases, the families K, L, and P dominate the graphs. Families of parabolic or of zero angular momentum orbits exist in the borders of the main families. Then, its possible to solve optimization problems. From the solutions of the optimum problems, we can find specific trajectories (escapes, captures, etc.) that contain variables that are extremized like the distance of the perigee and/or velocity at the perigee. In that way we can use these data to design specific missions.

ACKNOWLEDGMENT

The authors are grateful to the National Council for Scientific and Technological development (CNPq), Brazil, for the research grant receive under Contracts 300221/95-9 and to the Foundation to Support Research in the São Paulo State (FAPESP) for the research grant received under Contracts 1995/9290-1 and 97/13739-0.

REFERENCES

[1]SWENSON, B.L. (1992). "Neptune Atmospheric Probe Mission", AIAA Paper 92-4371.

[2]WEINSTEIN, S.S. (1992). "Pluto Flyby Mission Design Concepts for Very Small and Moderate Spacecraft", AIAA Paper 92-4372.

[3]FARQUHAR, R.W. & D.W. DUNHAM (1981). "A New Trajectory Concept for Exploring the Earth's Geomagnetic Tail", *Journal of Guidance, Control and Dynamics*, Vol. 4, No. 2, pp. 192-196.

[4]FARQUHAR, R., D. MUHONEN & L.C CHURCH (1985). "Trajectories and Orbital Maneuvers for the ISEE-3/ICE Comet Mission", *Journal of Astronautical Sciences*, Vol. 33, No. 3, pp. 235-254.

[5]EFRON, L., D.K. YEOMANS & A.F. SCHANZLE (1985). "ISEE-3/ICE Navigation Analysis," *Journal of Astronautical Sciences*, Vol. 33, No. 3, pp. 301-323.

[6]MUHONEN, D., S. DAVIS, & D. DUNHAM (1985). "Alternative Gravity-Assist Sequences for the ISEE-3 Escape Trajectory," *Journal of Astronautical Sciences*, Vol. 33, No. 3, pp. 255-273.

[7]FLANDRO, G. (1966). "Fast Reconnaissance Missions to the Outer Solar System Utilizing Energy

Derived from the Gravitational Field of Jupiter," *Astronautical Acta*, Vol. 12, No. 4.

[8]BYRNES, D.V. & L.A. D'AMARIO (1982) "A Combined Halley Flyby Galileo Mission," AIAA paper 82-1462. In: AIAA/AAS Astrodynamics Conference, San Diego, CA, Aug.

[9]D'AMARIO, L.A., D.V. BYRNES & R.H STANFORD. (1981). "A New Method for Optimizing Multiple-Flyby Trajectories, " *Journal of Guidance, Control, and Dynamics*, Vol. 4, No 6, pp. 591-596.

[10]D'AMARIO, L.A., D.V. BYRNES & R.H. STANFORD (1982). "Interplanetary Trajectory Optimization with Application to Galileo," *Journal of Guidance, Control, and Dynamics*, Vol. 5, No. 5, pp. 465-471.

[11]MARSH, S.M. & K.C. HOWELL (1988). "Double Lunar Swingby Trajectory Design," AIAA paper 88-4289.

[12]DUNHAM, D. & S. DAVIS (1985). "Optimization of a Multiple Lunar-Swingby Trajectory Sequence," *Journal of Astronautical Sciences*, Vol. 33, No. 3, pp. 275-288.

[13]PRADO, A.F.B.A. & R.A. BROUCKE (1994). "A Study of the Effects of the Atmospheric Drag in Swing-By Trajectories," *Journal of the Brazilian Society of Mechanical Sciences*, Vol. XVI, pp. 537-544.

[14]STRIEPE, S.A. & R.D. BRAUN (1991). "Effects of a Venus Swingby Periapsis Burn During an Earth-Mars Trajectory," *The Journal of the Astronautical Sciences*, Vol. 39, No. 3, pp. 299-312..

[15]FELIPE, G. & A.F.B.A. PRADO (1999). “Classification of Out of Plane Swing-by Trajectories”. *Journal of Guidance, Control and Dynamics*, Vol. 22, No. 5, pp. 643-649.

[16]PRADO, A.F.B.A. (1996). "Powered Swing-By". *Journal of Guidance, Control and Dynamics*, Vol. 19, No. 5, pp. 1142-1147.

[17]PRADO, A.F.B.A. & R.A. BROUCKE (1995). "A Classification of Swing-By Trajectories using The Moon". *Applied Mechanics Reviews*, Vol. 48, No. 11, Part 2, November, pp. 138-142.

[18]BROUCKE, R.A. (1988). "The Celestial Mechanics of Gravity Assist", AIAA Paper 88-4220.

[19] BROUCKE, R.A. & A.F.B.A. PRADO (1993). "Jupiter Swing-By Trajectories Passing Near the Earth", *Advances in the Astronautical Sciences*, Vol. 82, No 2, pp. 1159-1176.

[20]PRADO, A.F.B.A. (1993). "Optimal Transfer and Swing-By Orbits in the Two- and Three-Body Problems", Ph.D. Dissertation, Dept. of Aerospace Engineering and Engineering Mechanics, Univ. of Texas, Austin, TX.

[21]PRADO, A.F.B.A. (1997). "Close-approach Trajectories in the Elliptic Restricted Problem", *Journal of Guidance, Control, and Dynamics*, Vol. 20, No. 4, pp. 797-802.

[22]SZEBEHELY, V. (1967). *Theory of Orbits*, Academic Press, New York, Chap. 10.